SMC-TR-93-54

AEROSPACE REPORT NO.
TR-92(2940)-3

On the Theory of Morphology-Dependent Resonances: Shape Resonances, Width Formulas, and Graphical Representations

Prepared by

B. R. JOHNSON
Space and Environment Technology Center
Technology Operations

26 October 1993

Prepared for

SPACE AND MISSILE SYSTEMS CENTER
AIR FORCE MATERIEL COMMAND
2430 E. El Segundo Boulevard
Los Angeles Air Force Base, CA 90245

Engineering and Technology Group

THE AEROSPACE CORPORATION
El Segundo, California

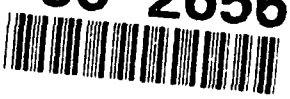

This report was submitted by The Aerospace Corporation, El Segundo, CA 90245-4691, under Contract No. F04701-93-C-0094 with the Space and Missile Systems Center, 2430 E. El Segundo Blvd., Los Angeles Air Force Base, CA 90245. It was reviewed and approved for The Aerospace Corporation by A. B. Christensen, Principal Director, Space and Environment Technology Center. Capt. Francis K. Chun was the project officer for the Mission-Oriented Investigation and Experimentation (MOIE) program.

This report has been reviewed by the Public Affairs Office (PAS) and is releasable to the National Technical Information Service (NTIS). At NTIS, it will be available to the general public, including foreign nationals.

This technical report has been reviewed and is approved for publication. Publication of this report does not constitute Air Force approval of the report's findings or conclusions. It is published only for the exchange and stimulation of ideas.

WM KYLE SNEDDON, Capt, USAF
Deputy Chief, Industrial & Int'l Division

FRANCIS K. CHUN, Capt, USAF
Deputy Chief, Brilliant Eyes Test & Mission Ops Branch

UNCLASSIFIED

SECURITY CLASSIFICATION OF THIS PAGE

REPORT DOCUMENTATION PAGE

1a. REPORT SECURITY CLASSIFICATION Unclassified	1b. RESTRICTIVE MARKINGS
2a. SECURITY CLASSIFICATION AUTHORITY	3. DISTRIBUTION/AVAILABILITY OF REPORT Approved for public release; distribution unlimited
2b. DECLASSIFICATION/DOWNGRADING SCHEDULE	
4. PERFORMING ORGANIZATION REPORT NUMBER(S) TR-92(2940)-3	5. MONITORING ORGANIZATION REPORT NUMBER(S) SMC-TR-93-54
6a. NAME OF PERFORMING ORGANIZATION The Aerospace Corporation Technology Operations 6b. OFFICE SYMBOL *(If applicable)*	7a. NAME OF MONITORING ORGANIZATION Space and Missile Systems Center
6c. ADDRESS *(City, State, and ZIP Code)* El Segundo, CA 90245-4691	7b. ADDRESS *(City, State, and ZIP Code)* Los Angeles Air Force Base Los Angeles, CA 90009-2960
8a. NAME OF FUNDING/SPONSORING ORGANIZATION 8b. OFFICE SYMBOL *(If applicable)*	9. PROCUREMENT INSTRUMENT IDENTIFICATION NUMBER F04701-88-C-0089
8c. ADDRESS *(City, State, and ZIP Code)*	10. SOURCE OF FUNDING NUMBERS PROGRAM ELEMENT NO. / PROJECT NO. / TASK NO. / WORK UNIT ACCESSION NO.

11. TITLE *(Include Security Classification)*
On the theory of morphology-dependent resonances: Shape resonances, width formulas and graphical representations

12. PERSONAL AUTHOR(S)
Johnson, B. Robert

13a. TYPE OF REPORT	13b. TIME COVERED FROM ____ TO ____	14. DATE OF REPORT *(Year, Month, Day)*	15. PAGE COUNT
		1993 October 26	42

16. SUPPLEMENTARY NOTATION

17. COSATI CODES			18. SUBJECT TERMS *(Continue on reverse if necessary and identify by block number)*
FIELD	GROUP	SUB-GROUP	Morphology-dependent resonance, Shape resonance, Mie scattering

19. ABSTRACT *(Continue on reverse if necessary and identify by block number)*

The theory of morphology-dependent resonances of a spherical particle is developed in analogy with the theory of quantum mechanical shape resonances. Exact analytic formulas for predicting the widths of the resonances are developed. A useful graphical procedure for organizing and displaying data for a spectrum of resonances is demonstrated.

20. DISTRIBUTION/AVAILABILITY OF ABSTRACT	21. ABSTRACT SECURITY CLASSIFICATION
[X] UNCLASSIFIED/UNLIMITED [ ] SAME AS RPT. [ ] DTIC USERS	Unclassified

22a. NAME OF RESPONSIBLE INDIVIDUAL	22b. TELEPHONE *(Include Area Code)*	22c. OFFICE SYMBOL

DD FORM 1473, 84 MAR

83 APR edition may be used until exhausted.
All other editions are obsolete.

SECURITY CLASSIFICATION OF THIS PAGE
UNCLASSIFIED

PREFACE

This report presents the results of work sponsored by the USAF Space and Missile Systems Center under Contract No. F04701-88-C-0089.

CONTENTS

FIGURES

1. INTRODUCTION

The cross section for scattering electromagnetic energy by a dielectric sphere exhibits a series of sharp peaks as a function of the size parameter. These peaks are a manifestation of scattering resonances in which electromagnetic energy is temporarily trapped inside the particle. A physical interpretation is that the electromagnetic wave is trapped by almost total internal reflection as it propagates around the inside surface of the sphere, and after circumnavigating the sphere, the wave returns to its starting point in phase. These resonances are now generally referred to as morphology-dependent resonances (MDRs). A large body of literature has been written on the subject. A good review article, containing many references to the original literature, has recently been written by Hill and Benner.[1]

MDRs are responsible for the ripple structure observed in Mie scattering[2] and for the large optical feedback necessary for lasing,[3,4] stimulated Raman scattering,[5] sum-frequency generation,[6] and other nonlinear processes that have been observed in small droplets. Stimulated Raman scattering from small spheres has been proposed as a method for analyzing the chemical concentration and size of droplets in fuel sprays,[7] and the elastic scattering of light near an MDR has been used to determine chemical composition of aerosol particles.[8] MDRs are also responsible for enhanced energy transfer that has been observed in aerosol particles.[9] Laboratory demonstrations have recently shown that the MDRs of an ensemble of microspheres can be utilized to construct a new type of optical memory.[10]

The present paper covers three topics in the theory of MDRs. These are (i) an interpretation of MDRs as "shape resonances;" (ii) the derivation of exact analytic formulas for predicting the widths of resonances; and (iii) the demonstration of a useful graphical procedure for displaying resonance data. The theory of shape resonances is a familiar topic in atomic and molecular scattering theory; however, the fact that MDRs can be regarded as shape resonances does not seem to be widely appreciated. In this interpretation, the electromagnetic energy is temporarily trapped near the surface of the sphere in a "dielectric potential well." The energy enters and exits the well by tunneling through a centrifugal barrier. Recently this problem has been studied using complex angular momentum theory.[11,12]

This report is organized as follows. Section 2 begins with a review of some of the basic equations for electromagnetic scattering from spherically symmetric particles. This section is presented mainly as a matter of convenience. It helps to establish our conventions and notation and also gathers together equations that will be needed later. Section 3 discusses resonance theory and shows how MDRs can be interpreted as shape resonances. Also included in this section is a related discussion of electromagnetic bound states in negative dielectric particles. In Section 4, several new exact analytic formulas for predicting the widths of resonances are developed. Formulas are derived for both real and complex indices of refraction. In Section 5, a useful graphical procedure for organizing and displaying the data for a spectrum of resonances is presented. Section 6 includes a summary and concluding remarks.

2. SCATTERING THEORY

This section briefly reviews the theory of electromagnetic scattering from a spherical particle. The basic equations needed in the remainder of the report are presented, and some of the conventions and the notation to be used are established. The particle is assumed to be nonmagnetic. The radius of the particle is denoted by a and the complex index of refraction, which may be a function of the radial coordinate r, is denoted by $m(r) = m_r(r) + im_i(r)$. In the region outside the sphere, $r > a$, the index of refraction is m(r) = 1, and the wave number is $k = 2\pi/\lambda$. The complex time dependence of the electric field is exp(-iωt). This time-dependence convention is the same as that used by Bohren and Huffman,[13] but is opposite of that used by Van de Hulst[14] and Kerker[15]. With this convention, a positive imaginary part of the index of refraction results in power absorption by the particle.

The electric field must satisfy the scattering boundary conditions and the following vector wave equation

$$\nabla \times \nabla \times \mathbf{E} - k^2 m^2(r)\mathbf{E} = 0 \,. \tag{1}$$

The solution to this equation is most easily computed by expanding the electric field in terms of the spherical vector wave functions,

$$\mathbf{M}_{n,m}(r,\theta,\phi) = \frac{\exp(im\phi)}{kr} S_n(r)\mathbf{X}_{n,m}(\theta)$$

$$\mathbf{N}_{n,m}(r,\theta,\phi) = \frac{\exp(im\phi)}{k^2 m^2(r)}\left[\frac{1}{r}\frac{\partial T_n(r)}{\partial r}\mathbf{Y}_{n,m}(\theta) + \frac{1}{r^2}T_n(r)\mathbf{Z}_{n,m}(\theta)\right], \tag{2}$$

where the functions $\mathbf{M}_{n,m}(r,\theta,\phi)$ are the transverse electric (TE) modes, and the functions $\mathbf{N}_{n,m}(r,\theta,\phi)$ are the transverse magnetic (TM) modes. The angular functions in these expressions are defined as

$$\mathbf{X}_{n,m}(\theta) = i\pi_{n,m}(\theta)\hat{\mathbf{e}}_\theta - \tau_{n,m}(\theta)\hat{\mathbf{e}}_\phi$$

$$\mathbf{Y}_{n,m}(\theta) = \tau_{n,m}(\theta)\hat{\mathbf{e}}_\theta - i\pi_{n,m}(\theta)\hat{\mathbf{e}}_\phi$$

$$\mathbf{Z}_{n,m}(\theta) = n(n+1)P_n^m(\cos\theta)\hat{\mathbf{e}}_r\,, \tag{3}$$

where

$$\pi_{n,m}(\theta) = \frac{m}{\sin\theta}P_n^m(\cos\theta)$$

$$\tau_{n,m}(\theta) = \frac{\partial}{\partial\theta}P_n^m(\cos\theta)\,. \tag{4}$$

The function $P_n^m(\cos\theta)$ is the associated Legendre polynomial, and $\hat{\mathbf{e}}_r, \hat{\mathbf{e}}_\theta, \hat{\mathbf{e}}_\phi$ are the unit orthogonal vectors associated with spherical coordinates. The functions $S_n(r)$ and $T_n(r)$ are the radial Debye potentials, which satisfy the following second order differential equations[16,17]

$$\frac{d^2S_n(r)}{dr^2} + \left[k^2m^2(r) - \frac{n(n+1)}{r^2}\right]S_n(r) = 0 \tag{5a}$$

$$\frac{d^2T_n(r)}{dr^2} - \frac{2}{m(r)}\frac{dm(r)}{dr}\frac{dT_n(r)}{dr} + \left[k^2m^2(r) - \frac{n(n+1)}{r^2}\right]T_n(r) = 0. \tag{5b}$$

The solutions to these equations must obey the initial conditions $S_n(0) = 0$ and $T_n(0) = 0$. These conditions are necessary to ensure that the electric field is finite at the origin.

In regions where the index of refraction has the constant value m, the two differential equations (5a,b) have the same form, and the linearly independent solutions are Riccati-Bessel functions,[18] which are defined as

$$\psi_n(mkr) = mkr\, j_n(mkr) \tag{6a}$$

$$\chi_n(mkr) = mkr\, n_n(mkr)\ , \tag{6b}$$

where $j_n(mkr)$ and $n_n(mkr)$ are spherical Bessel functions. In the external region, $r \geq a$, where $m(r) = 1$, the general solutions are linear combinations of the Riccati-Bessel functions. For later use in this report, it will be convenient to define these external solutions as follows:

$$S_n(r) = B_n\left[\chi_n(kr) + \beta_n \psi_n(kr)\right] \tag{7a}$$

$$T_n(r) = A_n\left[\chi_n(kr) + \alpha_n \psi_n(kr)\right], \tag{7b}$$

where α_n, β_n, A_n and B_n are constants. These functions must connect, in an appropriate manner, at the surface of the sphere, with the solutions inside the sphere. The connection of the internal and external solutions is most easily carried out using the log derivative formalism.

The "modified log derivative functions" of $S_n(r)$ and $T_n(r)$ are defined as

$$U_n(r) = \frac{1}{k}\left[S_n'(r) / S_n(r)\right] \tag{8a}$$

$$V_n(r) = \frac{1}{km^2(r)}\left[T_n'(r) / T_n(r)\right], \tag{8b}$$

where the prime denotes the derivative with respect to the argument of the function. Both of these functions are continuous at all points. This includes points where the index of refraction is

discontinuous, such as at the surface of the sphere or, in the case of a layered sphere, at the boundaries between the layers. It will also be useful to define the log derivatives of the Riccati-Bessel functions by the relations

$$D_n(x) = \psi_n'(x) / \psi_n(x) \tag{9a}$$

$$G_n(x) = \chi_n'(x) / \chi_n(x) \tag{9b}$$

Substitute the external solutions defined by (7) into the definitions of the modified logarithmic derivatives given by (8) and evaluate at the surface of the sphere. Then use the continuity of the functions $U_n(r)$ and $V_n(r)$ across the boundary to obtain

$$U_n(a) = \frac{\chi_n'(ka) + \beta_n \psi_n'(ka)}{\chi_n(ka) + \beta_n \psi_n(ka)} \tag{10a}$$

$$V_n(a) = \frac{\chi_n'(ka) + \alpha_n \psi_n'(ka)}{\chi_n(ka) + \alpha_n \psi_n(ka)} . \tag{10b}$$

where $U_n(a)$ and $V_n(a)$ are evaluated from the internal solution. These equations can be solved for α_n and β_n. The results are

$$\beta_n = -\frac{\chi_n(ka)}{\psi_n(ka)}\left[\frac{G_n(ka) - U_n(a)}{D_n(ka) - U_n(a)}\right] \tag{11a}$$

$$\alpha_n = -\frac{\chi_n(ka)}{\psi_n(ka)}\left[\frac{G_n(ka) - V_n(a)}{D_n(ka) - V_n(a)}\right] . \tag{11b}$$

For the special case of Mie scattering, in which the index of refraction has a constant value m, the solutions of the differential equations (5) in the region $0 \le r \le a$ are given by

$$S_n(r) = T_n(r) = \psi_n(mkr) \ . \tag{12}$$

Substitute these functions into (8) to obtain

$$U_n(r) = mD_n(mkr) \tag{13a}$$

$$V_n(r) = \frac{1}{m} D_n(mkr) \ . \tag{13b}$$

These expressions are then substituted into (11) to obtain

$$\beta_n = -\frac{\chi_n(x)}{\psi_n(x)}\left[\frac{G_n(x) - mD_n(mx)}{D_n(x) - mD_n(mx)}\right] \tag{14a}$$

$$\alpha_n = -\frac{\chi_n(x)}{\psi_n(x)}\left[\frac{mG_n(x) - D_n(mx)}{mD_n(x) - D_n(mx)}\right], \tag{14b}$$

where $x = ka$ is the size parameter.

It can be shown that α_n and β_n are related to the a_n and b_n coefficients of Mie theory by the formulas

$$b_n = \frac{1}{1 - i\beta_n} \tag{15a}$$

and

$$a_n = \frac{1}{1 - i\alpha_n} \quad . \tag{15b}$$

The a_n and b_n coefficients defined here are the same as the coefficients defined in Bohren and Huffman[13] and are the complex conjugate of the coefficients defined by Van de Hulst[14] and by Kerker.[15] All the usual formulas for cross sections and other quantities that are expressed in terms of the a_n and b_n coefficients are applicable.

3. RESONANCE THEORY

3.1 QUANTUM MECHANICAL ANALOGY

The second-order differential equations (5) can be recast in a form similar to the radial Schrödinger equation. This well known analogy is useful because one can then formulate problems in such a way that familiar quantum mechanical techniques can be used. To simplify the analogy, assume that the Schrödinger equation is expressed in units such that $\hbar^2 / 2\mu = 1$ (where $\hbar$ is Plank's constant and μ is the reduced mass). The radial Schrödinger equation then has the form

$$-\frac{d^2\psi(r)}{dr^2} + \left[V(r) + \frac{n(n+1)}{r^2}\right]\psi(r) = E\psi(r)\,, \tag{16}$$

where $V(r)$ is the potential energy function and E is the total energy. Equation (5a) will be identical in form to the Schrödinger equation if we define the potential to be

$$V(r) = k^2[1 - m^2(r)] \tag{17}$$

and the energy to be

$$E = k^2\,. \tag{18}$$

[Equation (18) was obtained by comparing the equations for the case of free space, i.e., for $m(r) = 1$ and $V(r) = 0$.] We note immediately that one noteworthy difference between the quantum mechanical and electromagnetic cases is that, in the latter case, the potential function is directly proportional to the "energy" (i.e., to k^2) whereas in the former case $V(r)$ is usually a fixed function, independent of the energy. This difference will lead to some interesting consequences that will be discussed in section 3.3.

The "total potential" is the sum of the potential function, $V(r)$, and the "centrifugal" potential. It is given by

$$V_n(r) = k^2[1 - m^2(r)] + \frac{n(n+1)}{r^2}\,. \tag{19}$$

The local wave number, $p_n(r)$, is defined by the relation $p_n^2(r) = E - V_n(r)$. This can also be written in the form

$$p_n^2(r) = k^2 m^2(r) - \frac{n(n+1)}{r^2} . \tag{20}$$

The quantity $p_n^2(r)$ is analogous to the kinetic energy in quantum mechanics. A region is classically allowed or classically forbidden depending on whether $p_n^2(r)$ is positive or negative, respectively.

Consider the special case of a spherical particle with a constant index of refraction m. The potential, in this case, is given by

$$V_n(r) = \begin{cases} k^2(1-m^2) + n(n+1)/r^2 & r \le a \\ n(n+1)/r^2 & r > a . \end{cases} \tag{21}$$

Whether this potential is attractive or repulsive will depend on the values of both m^2 and k^2. The case of most interest in this report is that of a dielectric particle with $m^2 > 1$ and with $k^2 > 1$. (Other cases will be considered in Section 3.3.) As a specific example, consider the potential function $V_{40}(r)$ for a particle of radius a, index of refraction $m = 1.47$, and wave number $k = 33/a$. For convenience, we choose the unit of length to be equal to the particle radius. Thus, $a = 1.0$, and $k = 33$. The potential function, $V_{40}(r)$, for this case, is shown drawn to scale in Fig. 1. The most striking feature of this function is the presence of a potential well in the region $r_1 < r < a$. This is a classically allowed region in which $p_n^2(r) > 0$. The well is surrounded by the two classically forbidden regions $0 \le r < r_1$ and $a < r < r_2$ in which $p_n^2(r) < 0$. The points r_1 and r_2, defined by the relation $p_n^2(r) = 0$, are called the classical turning points.

In the equivalent quantum mechanical problem, a particle can tunnel through the classically forbidden region, $a < r < r_2$, into the classically allowed potential well. For certain values of the energy, the particles will become temporarily trapped in the well, oscillating back and forth many times before finally tunneling back through the classically forbidden region to the outside world again. These quasi-bound states are also known as resonances. The type of resonance described here is called a shape resonance. The name "shape resonance" means simply that the resonance behavior arises from the "shape" of the potential, i.e., the well and the barrier.[19] This particular type of shape resonance, in which the barrier is formed by the centrifugal potential, is also referred to as an orbiting resonance.[20] This latter name is particularly apt considering the usual interpretation of MDRs in terms of light rays propagating around the inside surface of the sphere.[1]

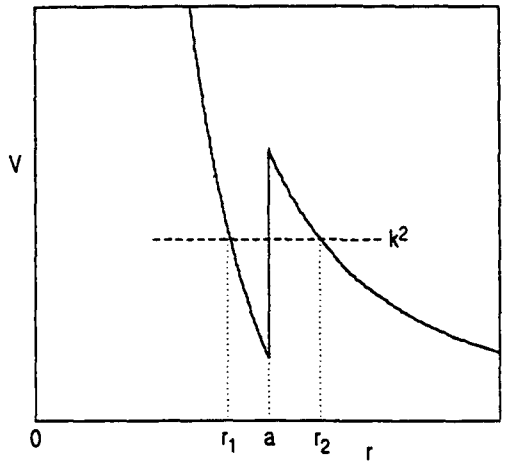

Figure 1. Effective potential associated with a spherical dielectric particle.

3.2 MDRs INTERPRETED AS SHAPE RESONANCES

The electromagnetic scattering problem is similar to the quantum mechanical problem. Electromagnetic energy can tunnel through the classically forbidden region and become temporarily trapped in resonance states. As we will demonstrate, these are the familiar morphology-dependent resonances (MDRs) predicted by Mie theory. In the following discussion, we will assume that the index of refraction is a real quantity.

In Fig. 1, the "energy" k^2 is approximately halfway between the top and bottom of the potential well. If the value of k^2 is changed, the shape of the potential well will also change. This is unlike the quantum mechanical problem where the potential is independent of the energy. As k is reduced in value, the bottom of the potential well will rise. For some value of k, the energy k^2 will coincide with the bottom of the potential well. We will refer to this energy as the bottom of the well and denote the value of k for which this occurs as k_B. The top of the well remains fixed in value as k^2 is varied. If k^2 is raised in value, it will eventually coincide with the top of the well. We will refer to this as the top of the well and denote the value of k for which this occurs as k_T.

The classical turning points are defined by the condition $p_n^2(r) = 0$. Solving Eq. (20) for this condition gives the two turning points,

$$r_1 = \frac{n+1/2}{km} \tag{22a}$$

$$r_2 = \frac{n+1/2}{k}, \tag{22b}$$

where we have replaced $[n(n+1)]^{1/2}$ with $n+1/2$ and used the fact that $m(r_1)=m$, and $m(r_2)=1$. These expressions for the turning points can be used to calculate the values of k_B and k_T. When $k=k_B$, the inner turning point must satisfy the relation $r_1=a$, and when $k=k_T$, the outer turning point must satisfy the relation $r_2=a$. Substituting these conditions into Eqs. (22) and solving for k gives $k_B=(n+1/2)/ma$, and $k_T=(n+1/2)/a$. It is more convenient to express these relations in terms of the dimensionless size parameter $x=ka$ rather than k. Thus, the condition for the bottom and top of the potential well is given by

$$x_B=\frac{n+1/2}{m} \tag{23a}$$

$$x_T=n+1/2. \tag{23b}$$

In quantum mechanics, only certain discrete energy levels are allowed in a one-dimensional potential well. The mathematical reason for this is that the boundary conditions can only be satisfied at these discrete energies. The problem of shape resonances is very similar. The resonances occur only for energy values that satisfy the boundary conditions, which are quite similar to the boundary conditions for the bound-state problem.

The boundary conditions at $r=0$ are given by $S_n(0)=T_n(0)=0$. These conditions, which we stated previously, must be met by all scattering solutions regardless of whether or not they are resonance states. The solutions that satisfy this condition are given by Eq. (12). The general form of the solutions in the region $r>a$ is given by Eq. (7). These functions are a linear combination of the Riccati-Bessel functions $\psi_n(kr)$ and $\chi_n(kr)$. In the classically forbidden region, $a<r<r_2$, these two functions have opposite behavior. The function $\psi_n(kr)$ exhibits a very rapid, "exponential-like" growth in this region while the function $\chi_n(kr)$ exhibits an "exponential-like" decrease. At $r=r_2$, these functions cease their exponential-like behavior and begin an oscillatory behavior in the region $r_2<r<\infty$.

The condition that determines the discrete energy levels of a quasibound shape resonance is the requirement that the wave function exhibit an exponential-like decay in the barrier region so that if the barrier extended to $r\rightarrow\infty$, the wave function would decay to zero, and the quasibound state would become a true bound state. This means that only the (exponential-like) decreasing function $\chi_n(kr)$ is allowed in the barrier region. Translating this requirement back to the wave functions defined by Eq. (7) implies that the coefficient that multiplies the (exponential-like) increasing function $\psi_n(kr)$ must be zero, i.e., $\beta_n=0$ ($\alpha_n=0$) at the location of a TE (TM) resonance, respectively. These conditions, which were obtained by satisfying the conditions for a shape resonance, are equivalent to the conditions commonly used to define the location of a morphology-dependent resonance.[1] This is evident from Eqs. (15a,b), which show that $\beta_n=0$ ($\alpha_n=0$) is equivalent to the condition that the imaginary part of the Mie coefficient b_n (a_n) be equal to zero.

Substituting $\beta_n = 0$ and $\alpha_n = 0$ into the Eqs. (14) give the following equations that must be satisfied at the locations of TE and TM resonances, respectively:

$$G_n(x_0) = mD_n(mx_0) \tag{24a}$$

$$mG_n(x_0) = D_n(mx_0)\ . \tag{24b}$$

A graphical illustration of these equations is quite illuminating. For this illustration, it is somewhat more convenient to work with the following functions;

$$d_n(mx) = D_n^{-1}(mx) \tag{25a}$$

$$g_n^{(TE)}(x) = mG_n^{-1}(x) \tag{25b}$$

$$g_n^{(TM)}(x) = \frac{1}{m}G_n^{-1}(x)\ . \tag{25c}$$

The conditions, given by Eqs. (24), for the TE and TM resonances are now expressed as

$$g_n^{(TE)}(x) = d_n(mx) \tag{26a}$$

$$g_n^{(TM)}(x) = d_n(mx). \tag{26b}$$

These functions are shown graphically in Fig. 2 for the case $m = 1.47$ and $n = 40$. The intersection points of the curves are the graphical solutions to the resonance equations. It is obvious from the graph that the $n = 40$ potential supports three TE and three TM resonances between the bottom and top of the potential well, $x_B = 27.5$ and $x_T = 40.5$. In addition, one can see from the graph that the size parameter for a TE resonance is always slightly less than for the equivalent TM resonance. An accurate computer solution of these equations gives the following

results: the TE resonances are located at 31.058854, 34.611195, and 37.653070 and the TM resonances are located at 31.519210, 34.996041, and 37.908035. The curves shown in Fig. 2 continue to intersect at an infinite number of points in the region $x > x_T$, i.e., above the top of the potential well. In general, the electromagnetic modes at these points are not counted as resonances because they are too wide to have the general properties associated with a resonance, such as a sharp spike in the scattering cross section. These "above the top of the well" states will be discussed further in Section 5.

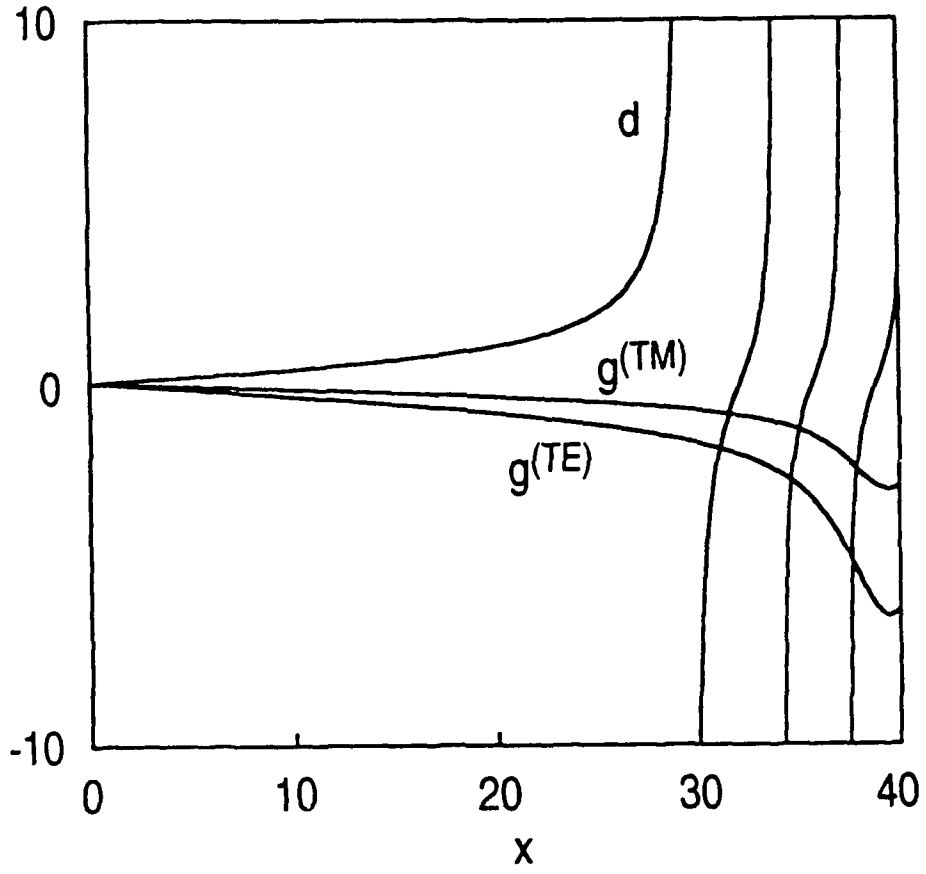

Figure 2. Graphical Solution to Eqs. (26a,b). Intersection points are the size parameters of the TE and TM resonances in the region between the bottom and top of the potential well.

The wave functions for the three TE resonances are shown graphically in Fig. 3. These wave functions are the Debye potential functions, $S_{40}(r)$, obtained by solving Eq. (5a). They are shown superimposed, at the proper level, on the potential function $V_{40}(r)$. Within the region of the potential well, these wave functions resemble bound states. The lowest level wave function has a single peak, the next level has two peaks (positive and negative), and the third level has three peaks. The number of peaks in the classically allowed region of the potential well , $r_1 \le r \le a$, is called the order number and is denoted by l. This number, along with the mode number n and the label TE or TM, uniquely identifies a resonance. Electromagnetic energy is temporarily trapped in the potential well. It can enter and leave by tunnelling through the outer centrifugal barrier of the potential well. The width of the resonance is inversely proportional to the lifetime of the trapped energy, which, in turn, is determined by the rate of tunneling through the barrier. The levels near the bottom of the well must tunnel through a larger barrier than the upper levels. Therefore, the lower levels have a longer lifetime and hence a narrower width than the upper levels. The widths of the three TE resonances (which were calculated using Eq. (34) in the following section) are 0.00008782, 0.01023, and 0.1297.

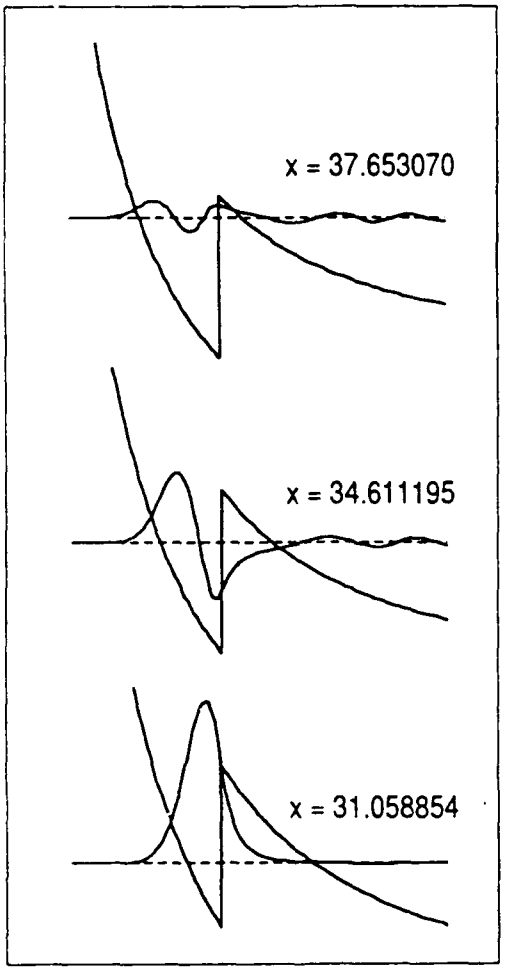

Figure 3. Radial wave functions for the three TE, n = 40 resonances.

Fig. 4 shows the dramatic change that the wave function experiences as the system traverses through the TE, $n = 40$, $l = 2$ resonance, located at $x_0 = 34.611195$. For graphical convenience, the particle radius is $a = 1.0$. The top panel of Fig. 4 shows the wave function for the case $x = 34.911195$, which is above the resonance. The wave function $S_{40}(r)$ is shown superimposed, at the proper level, on a plot of the potential function. The wave function shows an exponential-like increase in the tunneling region. Because of this growth, the amplitude of the wave function in the region $r > r_2$, outside the particle, is much greater than the amplitude inside the particle. The center panel shows the case $x = 34.611195$, which is on resonance. In this case, the wave function decays in an exponential-like manner in the tunneling region. This behavior is opposite from the previous case. The amplitude of the wave function inside the particle is now much larger than the amplitude outside. The result is that as one approaches the particle, the field strength increases rapidly in the region $a < r < r_1$, which is a layer just outside the surface, and then continues to rise to a maximum inside the particle near the surface. This increased field strength near the surface (both inside and outside the particle) is a characteristic resonance phenomenon. Finally, the bottom panel shows the case $x = 34.311195$, which is below the resonance. The behavior in this case is very similar to that in the top panel, i.e., the wave function increases exponential-like in the tunneling region, resulting in a small amplitude inside the particle relative to the amplitude outside. However, in this case, the exponential-like growth in the tunneling region is in the negative direction compared to the top panel. This results in a 180°

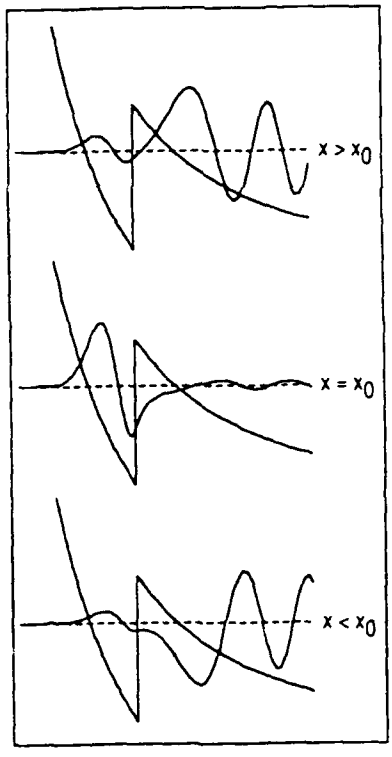

Figure 4. Behavior of the TE wave function in the vicinity of a resonance. The top panel shows the behavior for a size parameter value slightly above the resonance, the middle panel is on resonance, and the bottom panel is below the resonance.

phase shift of the outside wave function compared to its phase in the top panel. This 180^{o} phase shift is also a characteristic feature of a shape resonance.

The amplitudes of the wave functions shown in Figs. 3 and 4 cannot be directly compared with each other because each of these functions has been individually normalized to fit on the graph. To compare the peak amplitudes, it is necessary to normalize the wave functions so that they all have the same amplitude at $r \rightarrow \infty$. If we choose the wave amplitude at infinity to be 1, the following results are obtained: The peak amplitudes of the wave functions shown in Fig. 3 are (from top to bottom) 5.00, 18.67, and 225.25. The peak amplitudes (inside the particle) for the wave functions shown in Fig. 4 are (from top to bottom) 0.379, 18.67, and 0.274.

The picture that has been developed in this section, which portrays an MDR as a quasi-bound state, trapped in a potential well and connected to the outside world by tunneling, gives added intuition and insight into the nature of electromagnetic scattering resonances. This intuition is especially valuable for more complicated problems in which the particle has a layered structure[21] or a continuously varying index of refraction[22].

3.3 PARTICLES WITH NEGATIVE DIELECTRIC FUNCTIONS

The dielectric function, $\varepsilon(\omega)$, of many materials is negative over a portion of the frequency spectrum. Examples are metals in the range $\omega < \omega_p$, where ω_p is the plasma frequency and crystalline solids, such as NaCl, in the range $\omega_T < \omega < \omega_L$ where ω_T and ω_L are the transverse and longitudinal optical frequencies.[23] In this discussion, we will assume that the real part of the dielectric function is negative, and that the imaginary part is small and can be set equal to zero. The index of refraction is related to the dielectric function by $m^2 = \varepsilon$. Thus, at a frequency where $m^2 < 0$, the potential function given by Eq. (17) is a positive quantity.

As the first example case, consider a layered particle with a positive dielectric core covered by negative dielectric layer. The core has a radius $a_1 = 1.0$ and index of refraction $m_1 = 1.47$. The outer layer has a thickness $\Delta a = 0.05$ and index of refraction $m_2 = 0.8i$ (where i is the imaginary unit). The potential function, $V_n(r)$, for the case $n = 40$ and $k = 45$, is shown, plotted to scale in Fig. 5. The bottom of the potential well is $k_B = (n + 1/2)/m_1$. This is the same as in

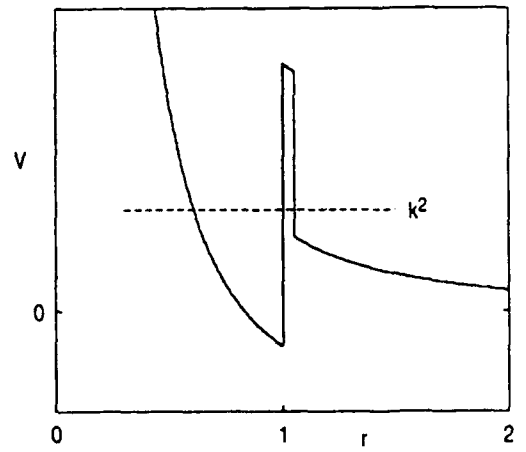

Figure 5. Effective potential function for a layered sphere with a positive dielectric core covered by a negative dielectric layer.

the previous example problem. However, there is no top to the potential well as defined previously. That is, there is no value k_T for which k^2 coincides with the top of the well. As the value of k^2 is increased, the top of the barrier also increases in such a manner that it always exceeds k^2. The wave function can tunnel through this barrier and become temporarily trapped in resonant states just as in the previous analysis.

Consider next a sphere composed entirely of a negative dielectric material. This is an interesting system because it has both scattering-state and bound-state solutions. This occurs because the potential defined by Eq. (17) changes from a repulsive barrier when $k^2 > 0$ to an attractive potential well when $k^2 < 0$. To illustrate this, consider a particle of radius $a = 1.0$ and index of refraction $m = 0.8i$. Fig. 6a shows the potential, $V_n(r)$, and the energy level, k^2, for the case $n = 40$ and $k = 45$. The potential forms a repulsive barrier that keeps the wave function from

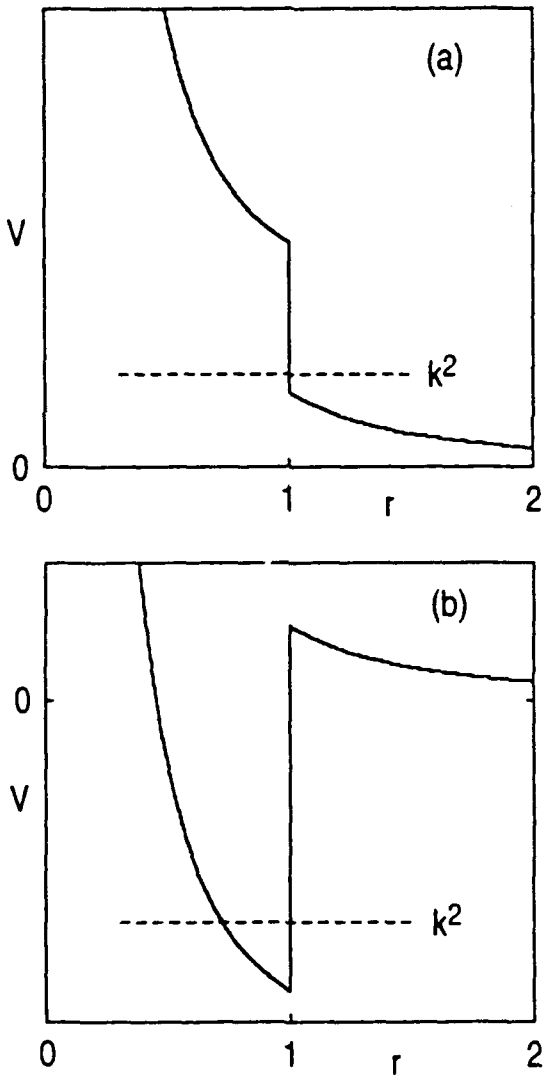

Figure 6. Effective potential associated with a negative dielectric particle. (a) the case $k^2 > 0$. (b) the case $k^2 < 0$.

penetrating beyond a skin depth into the particle. The region inside the particle is classically forbidden and the region outside is classically allowed. This situation is reversed if we let $k^2 < 0$. Then the classically allowed region is inside the particle, and the classically forbidden region is outside. This is shown in Fig 6b where the system is identical to that in Fig 6a with the exception that we now let $k = 70i$. Because $k^2 < 0$, the potential is negative. Thus, an attractive potential well is formed as shown. This situation is analogous to the quantum mechanical bound-state problem. Only selected eigenvalues of k^2 are allowed because the wave function must satisfy boundary conditions similar to those for resonances. The difference, in this case, is that the wave function cannot tunnel through a barrier, but must continue to decay exponentially to zero. Thus, these are true bound states. There is no radiative energy loss. (However, the inevitable internal energy loss that occurs in any real system will cause these modes to decay. In order for these modes to exist, there must be some mechanism to pump energy into them to replace the internal losses.) A part of the wave function penetrates into the forbidden region outside of the sphere to form an evanescent wave near the surface of the sphere.

The allowed eigenvalues of k can be computed in a manner analogous to that used to calculate the locations of the resonances. The spectrum of eigenvalues, $k_{n,l}^2$, forms a sequence of negative values that begins at the upper (least negative) value and decreases in quantized steps for l = 1,2,3,.... An upper bound to this sequence is obtained when k^2 coincides with the bottom of the potential well. This upper bound (which is a negative number) is given by

$$k_U^2 = \frac{n(n+1)}{m^2 a^2} . \tag{27}$$

For the example case we are considering, $k_U^2 = -2562.5$ (i.e., $k_U = 50.62i$). The spectrum of eigenvalues $k_{n,l}^2$ begins at a value below this upper bound and forms a decreasing sequence of quantized levels that continues without end. In quantum mechanics, the energy eigenvalues begin at a ground state near the bottom of the potential well and increase in quantized steps. At first sight, the present system does not seem to behave this way since the eigenvalues decrease in quantized steps. The reason for the apparent difference is because the bottom of the potential well is decreasing at an even faster rate than the eigenvalues $k_{n,l}^2$. Therefore, the interval between the levels $k_{n,l}^2$ and the bottom of the well actually increase in quantized steps exactly as in the quantum mechanical case.

4. RESONANCE WIDTHS

Useful analytic expressions for calculating resonance widths are derived in this section. These formulas cover the four cases involving TE and TM resonances for both real and complex indices of refraction.

4.1 TE RESONANCE, REAL INDEX OF REFRACTION

A TE resonance is characterized by a sharp peak in the real part of the $b_n(x)$ coefficient.[1] The resonance is located at a size parameter that satisfies the relation $\beta_n(x_0) = 0$. Since the index of refraction is real, it follows from Eq. (14a) that the function $\beta_n(x)$ is real. This fact, combined with Eq. (15a), gives the following expression for the real part of $b_n(x)$

$$\mathrm{Re}[b_n(x)] = \frac{1}{1+\beta_n^2(x)} . \tag{28}$$

At the center of the resonance this function has a maximum value $\mathrm{Re}[b_n(x_0)] = 1$, which drops off sharply on either side of x_0. The width of the resonance, $w_n(x_0)$, is defined to be the distance between the points $x_{\pm 1}$ on either side of x_0 where the amplitude has decreased to half its maximum value, i.e., to $\mathrm{Re}[b_n(x_{\pm 1})] = 1/2$. It follows from Eq. (28) that the half-amplitude points satisfy the relation $\beta_n^2(x_{\pm 1}) = 1$.

To a good approximation, the function $\beta_n(x)$ can be represented by the linear term of a Taylor series expansion around x_0,

$$\beta_n(x) = \beta_n'(x_0)(x - x_0), \tag{29}$$

where the prime denotes the derivative with respect to x. Within this linear approximation, the half amplitude points are $x_{\pm 1} = x_0 \pm \Delta x$, where $\beta_n'(x_0)\Delta x = 1$. Thus, the width is given by

$$w_n(x_0) = \frac{2}{\beta_n'(x_0)} . \tag{30}$$

Differentiate expression (14a) with respect to x and evaluate the result at x_0. The result is

$$\beta_n'(x_0) = -\frac{\chi_n(x_0)}{\psi_n(x_0)}\left[\frac{m^2 D_n'(mx_0) - G_n'(x_0)}{mD_n(mx_0) - D_n(x_0)}\right]. \tag{31}$$

This expression can be simplified with the aid of the following formulas

$$D_n'(x) = \frac{n(n+1)}{x^2} - 1 - D_n^2(x), \tag{32a}$$

$$G_n'(x) = \frac{n(n+1)}{x^2} - 1 - G_n^2(x), \tag{32b}$$

and

$$G_n(x) - D_n(x) = [\psi_n(x)\chi_n(x)]^{-1}. \tag{33}$$

The latter formula was obtained by use of the Wronskian relation for Riccati-Bessel functions.

Substitute the derivatives given by Eq. (32) into Eq. (31). Then use Eq. (24a) to replace $mD(mx_0)$ by $G(x_0)$. Finally, use Eq. (33) to simplify the result. The result of all this manipulation is a very simple expression for $\beta_n'(x_0)$, which can be substituted into Eq. (30) to give the following simple analytic formula for the width of a TE resonance:

$$w_n(x_0) = \frac{2}{(m^2 - 1)\chi_n^2(x_0)}. \tag{34}$$

4.2 TM RESONANCE, REAL INDEX OF REFRACTION

Using the same analysis as in the previous case, the following expression is obtained for the width of a TM resonance:

$$\overline{w}_n(x_0) = \frac{2}{\alpha_n'(x_0)}. \tag{35}$$

Differentiate expression (14b) to obtain

$$\alpha_n'(x_0) = -\frac{m\chi_n(x_0)}{\psi_n(x_0)}\left[\frac{G_n'(x_0) - D_n'(mx_0)}{mD_n(x_0) - D_n(mx_0)}\right]. \tag{36}$$

Equations (32), (33) and (24b) are then used to simplify this expression. Substitute the simplified result into Eq. (35) to obtain the following "exact" formula for the TM resonance

$$\overline{w}_n(x_0) = \frac{2}{(m^2-1)\chi_n^2(x_0)\left[\dfrac{n(n+1)}{m^2x_0^2} + G_n^2(x_0)\right]}. \tag{37}$$

4.3 TE RESONANCE, COMPLEX INDEX OF REFRACTION

If the index of refraction is allowed to become complex, the function $\beta_n(x)$, which depends parametrically on $m = m_r + im_i$, will also be complex. To explicitly indicate this dependence, we will write $\beta_n(m;x)$. The Taylor series expansion of $\beta_n(m;x)$, which was carried out previously with respect to the size parameter, x, can be extended to also include an expansion with respect to the index of refraction, m. The size parameter, x,will be expanded around the resonance point x_0, as in our previous analysis, and the index of refraction m will be expanded along the imaginary axis around the point $m = m_r$. The result is

$$\beta_n(m;x) = \beta_n'(m_r, x_0)(x - x_0) + i\gamma_n(m;x) \,. \tag{38}$$

where the imaginary component, $\gamma(m;x)$, is given by

$$\gamma_n(m;x) = m_i \times \left[\frac{\partial \beta_n(m;x)}{\partial m}\right]_{m=m_r} . \tag{39}$$

The subscript on the bracket in the above expression indicates that the derivative is to be evaluated at $m = m_r$.

Substitute the linear approximation (38) into Eq. (15a) and calculate the real part of $b_n(x)$. The result is

$$\mathrm{Re}[b_n(x)] = \frac{1+\gamma_n}{[1+\gamma_n]^2 + [\beta_n'(x - x_0)]^2} \,. \tag{40}$$

This function exhibits a resonance peak centered at x_0. Thus, the position of the resonance is not altered by adding a small imaginary component to the index of refraction. However, the maximum value of the resonance peak at x_0 is changed. Evaluating Eq. (40) at x_0 gives

$$\mathrm{Re}[b_n(x_0)] = \frac{1}{1+\gamma_n}. \tag{41}$$

The width of the resonance is defined to be the distance between the points where the amplitude has decreased to half of its maximum value. Thus,

$$\mathrm{Re}[b_n(x_0 \pm \Delta x)] = \frac{1}{2(1+\gamma_n)}, \tag{42}$$

The maximum amplitude of the resonance peak at x_0 is called the resonance height[24] and will be denoted by $H_n(m_i;x_0)$. Combine Eqs. (41) and (43) to obtain the following useful expression

$$H_n(m_i;x_0)=\frac{w_n(0;x_0)}{w_n(m_i;x_0)}\,. \tag{44}$$

This formula shows that the product of the height and width of the resonance is a constant, equal to the "undamped" width $w_n(0;x_0)$. The resonance height is a useful quantity because it is a measure of how much a resonance is suppressed by the internal energy absorption. If no energy is absorbed, the height has a maximum value of 1. If the height is very much less than 1, then the resonance is, for all practical purposes, suppressed out of effective existence.

Differentiate Eq. (14a) with respect to m to get

$$\frac{\partial\beta_n}{\partial m}=-\frac{\chi_n(x_0)}{\psi_n(x_0)}\left[\frac{D_n(mx_0)+mx_0D_n'(mx_0)}{mD_n(mx_0)-D_n(x_0)}\right]. \tag{45}$$

Use Eqs. (32), (33) and (24a) to simplify this expression. The result is

$$\frac{\partial\beta_n}{\partial m}=\frac{x_0\chi_0^2(x_0)}{m}\left\{[m^2-1]-[G_n'(x_0)+G_n(x_0)/x_0]\right\}. \tag{46}$$

Substitute this into Eq. (39) to get

$$\gamma_n(m;x_0)=\chi_n^2(x_0)(m_r^2-1)\frac{m_i}{m_r}[1-\varepsilon_n]x_0, \tag{47}$$

where ε_n is given by

$$\varepsilon_n=\frac{1}{(m_r^2-1)}\left[G_n'(x_0)+G_n(x_0)/x_0\right]. \tag{48}$$

Combine the results contained in expressions (34), (43) and (47) to obtain the following formula for the width of a TE resonance:

$$w_n(m_i;x_0) = w_n(0;x_0) + 2x_0\frac{m_i}{m_r}(1-\varepsilon_n). \tag{49}$$

The quantity ε_n can be evaluated by an approximate semiclassical WKB analysis. The result shows that $|\varepsilon_n| \approx O[1]/n$ where $O[1]$ is a number of order unity. Therefore, for most resonances $|\varepsilon_n| << 1$, and, to a good approximation, it can be neglected in Eq. (49). Thus, the final simplified result for the width of a TE resonance is

$$w_n(m_i;x_0) = \frac{2}{(m_r^2-1)\chi_n^2(x_0)} + 2x_0\frac{m_i}{m_r}. \tag{50}$$

The second term in the above expression, which is due to internal energy losses, sets a lower limit on the width of a resonance. This term was derived previously by Arnold using a physical argument based on a consideration of absorptive energy losses in a cavity.[9] It prevents the extremely narrow resonances that are sometimes predicted by theory when m_i is neglected. Eqs. (49) and (50) show that the width is a linear function of m_i, as has been previously reported.[24,25]

This result can be used in Eq. (44) to calculate the height of the resonance. It is apparent that, in cases where the undamped resonance width, $w_n(0;x_0)$, is extremely small, a small value of m_i can lead, for all practical purposes, to the complete suppression of the resonance.

4.4 TM RESONANCE, COMPLEX INDEX OF REFRACTION

The analysis of this case is identical to the previous case with α_n and a_n replacing β_n and b_n. Equation (14b) for $\alpha_n(m;x)$ must be differentiated with respect to m. The result, after simplifying with the aid of Eq. (24b), is

$$\frac{\partial\alpha_n}{\partial m} = -\frac{\chi_n(x_0)}{\psi_n(x_0)}\left[\frac{x_0D_n'(mx_0)-G(x_0)}{G(x_0)-D(x_0)}\right]. \tag{51}$$

This result can be further simplified with the use of Eqs. (33), (32a) and (24b). The result is

$$\frac{\partial \alpha_n}{\partial m} = \frac{\chi_n^2(x_0)}{m}\left[x_0 + m^2 x_0 G_n^2(x_0) - \frac{n(n+1)}{m^2 x_0}\right]. \tag{52}$$

Then, with the aid of expressions (37) and (43), we obtain the following formula for the width of the TM resonance:

$$\overline{w}_n(m_i; x_0) = \overline{w}_n(0; x_0) + 2x_0 \frac{m_i}{m_r}(1 - \overline{\varepsilon}_n), \tag{53}$$

where

$$\overline{\varepsilon}_n = \frac{G_n'(x_0) - G_n(x_0)/x_0}{(m^2 - 1)\left[G_n^2(x_0) + \dfrac{n(n+1)}{m^2 x_0^2}\right]}. \tag{54}$$

Similar remarks apply to the quantity $\overline{\varepsilon}_n$ as applied to the quantity ε_n defined by Eq. (48). For most resonances, $|\overline{\varepsilon}_n| << 1$ and can be neglected. Therefore, the final simplified result for the width of a TM resonance is

$$\overline{w}_n(m_i; x_0) = \frac{2}{(m_r^2 - 1)\chi_n^2(x_0)\left[\dfrac{n(n+1)}{m_r^2 x_0^2} + G_n^2(x_0)\right]} + 2x_0 \frac{m_i}{m_r}. \tag{55}$$

5. GRAPHICAL REPRESENTATION OF THE RESONANCE SPECTRUM

Each of the scattering resonances of a spherical particle is characterized by several parameters. These include the mode number, n, the order number, l, the size parameter, x_0, the width, $w_n(m_i;x_0)$, and the height, $H_n(m_i;x_0)$. It is useful to organize and present these data in such a way that one can see global patterns that relate and correlate the parameters for the various resonances. The most useful way of seeing these patterns is by a graphical display of the data.

Consider a two-dimensional diagram. The horizontal axis represents the mode number, n, and the vertical axis represents the parameter z, which is defined by

$$z = x - n/m, \tag{56}$$

where x is the size parameter. Recall that the bottom and top of the potential well are given by $x = (n+1/2)/m$ and $x = (n+1/2)$, respectively [see Eqs. (23)]. Thus, the bottom of the potential well is represented by the horizontal line $z = 1/(2m)$, and the top of the well is represented by the line $z = (1-1/m)n + 1/2$. Each resonance appears as a unique point in the $n-z$ plane. Most of these points fall in the wedge-shaped area between the lines representing the top and bottom of the well. (A few resonances may lie above the top of the well; we will discuss these later.) We can then draw a series of smooth curves through the points that represent resonances with the same order number, l. We will refer to these as the "resonance curves". The resonance curve for a given value of l defines a function of n, which we represent by $Z_l(n)$.

All this is illustrated in Fig. 7 where we show the TE resonances that fall in the range $1 < n < 200$ for a spherical particle with index of refraction $m = 1.47$. The heavy straight line

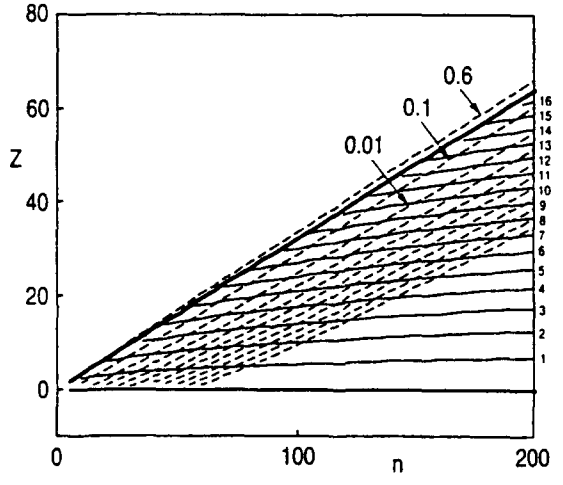

Figure 7. Graphical representation of TE resonance parameters for a spherical particle with index of refraction m = 1.47. The resonances are located at points on the solid curves corresponding to integer values of n. Each curve represents the resonances of a given order number. The dashed curves are contours of constant width. The heavy straight lines represent the top and bottom of the potential well.

segments that represent the top and bottom of the potential well can be easily identified in the graph. The 16 solid curves are the resonance curves $Z_l(n)$. The order numbers that label these curves are listed on the right side of the graph. The resonances are located at the points of intersection of the resonance curves with vertical lines that pass through the integer-valued points on the n axis.

The TE width Eq. (34) assigns a width to each point in the $n-z$ plane. This defines a surface on which contour lines of constant width can be established. These contours are the dashed-line curves in Fig. 7. The 11 contours shown are for the width values $w=0.6$ and $w_j=10^{-j}$ where $j=1,2,\cdots 10$. The contours 0.6, 0.1, and 0.01 have been labeled; the remaining contours follow in consecutive order. (Note that the contour for the width 0.6 is above the top of the well. This will be discussed in more detail later.) These curves define a set of functions that we represent by $F_w(n)$.

Approximate analyitic formulas can be written for the resonance curves, $Z_l(n)$, and the width contours, $F_w(n)$. The formula for the resonance curves is obtained directly from from an asymptotic expression for resonance frequencies derived by Schiller and Byer[26] [See Eq. 2 in reference 26]. The result is

$$Z_l(n)=\frac{1}{2m}-\frac{\zeta_l}{m}\left(\frac{n+1/2}{2}\right)^{1/3}-\frac{p}{\sqrt{m^2-1}}+\frac{3\zeta_l^2}{2^{2/3}10m(n+1/2)^{1/3}}$$

$$+\frac{m^2p(2p^2/3-1)\zeta_l}{2^{1/3}(m^2-1)^{3/2}(n+1/2)^{2/3}} \qquad 57)$$

where p = 1 for TE modes, p = $1/m^2$ for TM modes, and ζ_l denotes the l th zero of the Airy function Ai(ζ).

The width contour functions, $F_w(n)$, can be derived from the formulas for resonance widths developed by Probert-Jones[27] [See Eqs. (4) and(5) in reference 27]. These formulas all have the form

$$w_n=A(n,u)\exp\left[-\frac{4u}{3}\left(\frac{2u}{n+1/2}\right)^{1/2}\right], \qquad (58)$$

where the pre-exponential factor $A(n,u)$ is slowly varying compared to the exponential factor. The parameter u in this formula is defined by $u=(n+1/2)-x$, i.e., it is the distance of the resonance below the top of the well. Thus, it is complementary to our parameter z, which essentially measures the distance of the resonance above the bottom of the potential well. The relation between z and u is given by $z=(n+1/2)-n/m-u$.

If we neglect the effect of the pre-exponential factor in Eq. (58), then it is easy to see that the width will remain constant along a curve defined by the relation $u(n) = C_w(n+1/2)^{1/3}$, where C_w is a constant. Transforming to z, we obtain our expression for the width contours,

$$F_w(n) = (n+1/2) - n/m - C_w(n+1/2)^{1/3} \tag{59}$$

In this work, we have chosen to only deal with resonances that lie in a range between the top and bottom of the potential well. Previously, we noted that some resonances may have size parameters that lie slightly above the top of the potential well. Actually, the formulas (24) that define the size parameters of the resonances have solutions, $x_{n,l}$, which extend to infinity. If the graph in Fig. 2 were extended to the right, the curves $g_n^{(TE)}(x)$ and $g_n^{(TM)}(x)$ would continue to intersect the curve $d_n(mx)$ indefinitely, with each intersection point representing a solution to the resonance condition. However, most of the formal solutions that lie above the top of the well do not qualify as physically meaningful resonances because they are too wide. The width of any of these predicted resonances can be calculated by the analytic formulas (34) or (37), which are valid for all values of the size parameter. It is somewhat a matter of judgment, depending on the problem, to decide where to set an upper limit to the width. Hill and Benner chose to set the limit at $w = 0.6$ for a problem very similar to our example problem. This contour, which lies very slightly above the top of the well, is shown in Fig. 7. Very few resonances fall in the region between the top of the well and the $w = 0.6$ contour. Resonances above the top of the well are broad because there is no classically forbidden tunneling region that acts as a barrier to trap the energy.

Figure 7 shows results for the case in which the imaginary component of the index of refraction is zero. Adding a small imaginary component to the index of refraction will not affect the resonance curves, but will have a large effect on the widths and heights of the very narrow resonances. To illustrate this, consider the case in which the index of refraction is $m = 1.47 + i10^{-6}$. We have evaluated the TE resonance widths using Eq. (50). The width contours are shown in Fig. 8. These should be compared to the contours in Fig. 7.

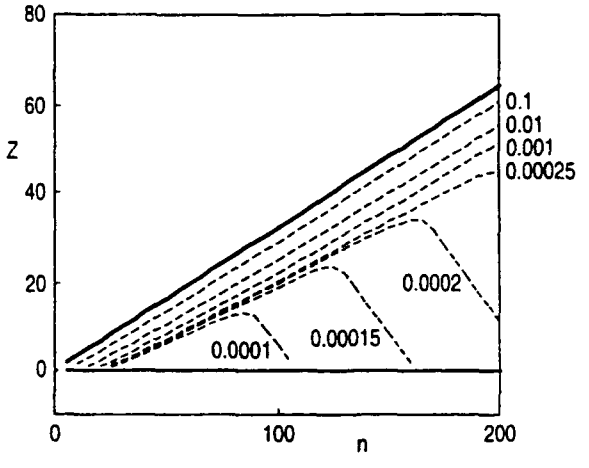

Figure 8. Width contours for TE resonances of a particle with a complex index of refraction m = 1.47 + i 0.000001.

The height of a resonance is defined in Section 4 as the maximum value of the function $\mathrm{Re}[b_n(x)]$ (or $\mathrm{Re}[a_n(x)]$) at the center of the resonance. (This quantity is also equal to the amplitude of the Mie coefficient $|b_n(x_0)|$ (or $|a_n(x_0)|$ at resonance). The height is 1.0 when the index of refraction is real, i.e. when $m_i = 0$. The height is less that 1.0 and given by the ratio of the widths as expressed in Eq. (44) when $m_i \neq 0$. This is an important quantity because it gives an indication of the strength of the resonance. If the height is 1.0, the resonance has maximum effectiveness in causing an enhancement of the cross section or in creating intense internal electric fields in the particle. If the height is less than 1.0, the effectiveness of the resonance is reduced, and, if it is much less that 1.0, the resonance is essentially damped out of effective existence. Contours of constant "resonance height" for our example problem are shown in Fig. 9. The height contours shown are 0.9, 0.5, 0.1, and 0.01. The resonances with heights greater than 0.9 are essentially full strength. The resonances with heights less than 0.01 are essentially suppressed out of existence for most applications.

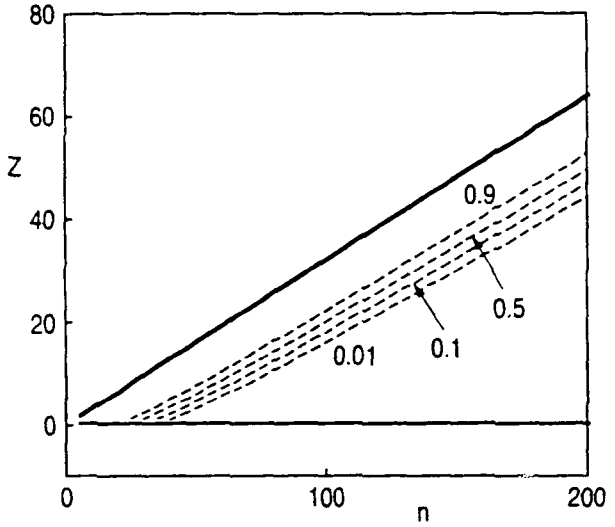

Figure 9. Height contours for the TE resonances of a particle with complex index of refraction m = 1.47 + i 0.000001.

6. SUMMARY AND CONCLUDING REMARKS

The analogy between the radial Schrödinger equation and the differential equations for the radial Debye potentials has been exploited for the purpose of analyzing electromagnetic scattering resonances. These resonances are shown to be analogous to quantum mechanical shape resonances. The picture developed in this report views these resonances as quasi-bound states, temporarily trapped in a potential well of the type illustrated in Fig. 1. This viewpoint provides some immediate intuitive insights into the nature of these resonances. For example, the top and bottom of the potential well determine effective upper and lower bounds for the resonance levels. The resonance widths, which are inversely proportional to the decay time of the quasi-bound state, are determined by the rate at which energy can tunnel through the outer barrier of the potential well. Since the lower levels must tunnel through a larger barrier, the lower levels have a longer lifetime and, thus, have narrower widths than the upper levels.

The condition that defines a shape resonance is similar to the condition that defines a bound state in a potential well. This condition states that the wave function must decrease "exponentially" in the classically forbidden regions outside the well. The application of this boundary condition leads directly to Eqs. (24a) and (24b). These are the same equations that have been derived in the theory of morphology-dependent resonances.[1] Figures 3 and 4 show the dramatic change that occurs in the wave function at resonance. These graphs show how the exponential behavior of the wave function in the classically forbidden region is responsible for the large electric-field amplitudes near the surface of a particle at resonance.

The interpretation of resonances as the quasi-bound states of a potential well can be applied to more complicated systems than a simple dielectric sphere. We briefly described one such system, a layered sphere with a negative dielectric outer layer. (The potential function for this case is illustrated in Fig. 5.) It is obvious that one can use a similar analysis to consider more complicated problems in which the particle has a multilayered structure[21] or a continuously varying index of refraction[22]. This approach offers intuitive insights to these more complicated resonance problems that are not available in the traditional picture, which views a resonance as a wave propagating around the sphere, confined by internal reflections.[1]

We have also used this analysis to briefly describe the very interesting case of a negative dielectric sphere. This problem is interesting because the system has two distinct types of solutions. We refer to these as the positive energy ($k^2 > 0$) and negative energy ($k^2 < 0$) solutions. For the positive energy solution, the potential in the interior of the particle is a repulsive barrier (illustrated in Fig. 6a) that keeps the wave function outside. This is a traditional scattering problem that can be calculated by Mie theory. For the negative energy solution, the potential inside the particle is a deep well (illustrated in Fig. 6b). This case is not a resonance problem, but it is very similar and can be analyzed by the same methods used to study resonances. In this case, the energy cannot tunnel out of the well; therefore, the electromagnetic modes are true bound states. If it were not for the inevitable internal losses, these states would have an infinite lifetime. These modes exist inside the particle with only a surface evanescent wave penetrating outside of the particle.

Exact analytic formulas for resonance widths were developed in Section 4 . The final useful and simplified results are contained in the two Eqs. (50) and (55). These formulas predict the widths of TE and TM resonances, respectively, for both complex ($m_i \neq 0$) and real ($m_i = 0$) indices of refraction. Another useful result of this section is the definition and discussion of the significance of the resonance height. The formula for the height is given by Eq. (44).

In Section 5, we presented graphical representations that we have found useful for correlating the position, width (see Figs. 7 and 8), and height data (Fig. 9) for a spectrum of resonances.

REFERENCES

1. S. C. Hill and R. E. Benner, "Morphology-dependent resonances," in *Optical Effects Associated with Small Particles* P. W. Barber and R. K. Chang, eds. (World Scientific. Singapore, 1988).

2. P. Chylek, "Particle-wave resonances and the ripple structure in the Mie normalized extinction cross section," J. Opt. Soc. Am. **66**, 285-287 (1976).

3. H.-M. Tzeng, K.F. Wall, M. B. Long, and R. K. Chang, "Laser emission from individual droplets at wavelengths corresponding to morphology-dependent resonances," Opt. Lett. **9**, 499-501 (1984).

4. S.-X. Qian, J. B. Snow, H.-M. Tzeng, and R. K. Chang, "Lasing droplets: highlighting the liquid-air interface by laser emission," Science **231**, 486-488 (1986).

5. J. R. Snow, S.-X. Qian and R. K. Chang, "Stimulated Raman scattering from individual water and ethanol droplets at morphology-dependent resonances," Opt. Lett. **10**, 37-39 (1985).

6. W. P. Acker, D. H. Leach and R. K. Chang, "Third-order optical sum-frequency generation in micrometer-sized droplets," Opt. Lett. **14**, 402-404 (1989).

7. W. P. Acker, A. Serpengüzel, R. K. Chang and S. C. Hill, "Stimulated Raman scattering of fuel droplets: chemical concentration and size determination," Appl. Phys. B **51**, 9-16 (1990).

8. S. Arnold, E. K. Murphy and G. Sager, "Aerosol particle molecular spectroscopy," Appl. Opt. **24**, 1048-1053 (1985).

9. L. M. Folan, S. Arnold and S. D. Druger, "Enhanced energy transfer within a microparticle," Chem. Phys. Lett. **118**, 322-327 (1985).

10. S. Arnold, C. T. Liu, W. B. Whitten and J. M. Ramsey, "Room-temperature microparticle-based persistent hole burning memory," Opt. Lett. **16**, 420-422 (1991).

11. H. M. Nussenzveig, "Tunneling effects in diffractive scattering and resonances," Comments Atomic and Molec. Phys. **23**, 175-187 (1989).

12. L. G. Guimarães and H. M. Nussenzveig, "Theory of Mie resonances and ripple fluctuations," Optics Commun. 89, 363-369 (1992). (This paper was published after the work for the present report was completed.)

13. C. F. Bohren and D. R. Huffman, *Absorption and Scattering of Light by Small Particles* (Interscience, New York, 1983).

14. H. C. van de Hulst, *Light Scattering by Small Particles* (Dover, New York, 1981).

15. M. Kerker, *The Scattering of Light and Other Electromagnetic Radiation* (Academic Press, New York, 1969).

16. C. T. Tai, *Dyadic Greens Functions in Electromagnetic Theory* (Intext Educational Publishers, Scranton PA, 1971).

17. P. J. Wyatt, "Scattering of electromagnetic plane waves from inhomogeneous spherically symmetric objects," Phys. Rev. **127**, 1837-1843 (1962).

18. M. Abramowitz and I. A. Stegun, eds. *Handbook of Mathematical Functions* (Dover, New York, 1965).

19. J. L. Dehmer, "Shape resonances in molecular fields," in *Resonances in Electron-Molecule Scattering, van der Waals Complexes, and Reactive Chemical Dynamics,* D. G. Truhlar ed. (American Chemical Society, Washington D. C., 1984).

20. J. P. Toennies, W. Weiz and G. Wolf, "Observation of orbiting resonances in H_2 - rare gas scattering," J. Chem. Phys. **64**, 5305-5307 (1976).

21. R. L. Hightower and C. B. Richardson, "Resonant Mie scattering from a layered sphere," Appl. Opt. **27**, 4850-4855 (1985).

22. D. Q. Chowdhury, S. C. Hill and P. W. Barber, "Morphology-dependent Resonances in radially inhomogeneous spheres," J. Opt. Soc. Am. A **8**, 1702-1705 (1991).

23. C. Kittel, *Introduction to Solid State Physics* (Wiley, New York, Fifth edition, 1976).

24. B. A. Hunter, M. A. Box and B. Maier, "Resonance structure in weakly absorbing spheres," J. Opt. Soc. Am. A **5**, 1281-1286 (1988).

25 G. J. Rosasco and H. S. Bennett, "Internal field resonance structure: Implications for optical absorption and scattering by microscopic particles," J. Opt.Soc. Am. **68**, 1242-1250 (1978).

26. S. Schiller and R. L. Byer, "High-resolution spectroscopy of whispering gallery modes in large dielectric spheres," Opt. Lett. **16**, 1138-1140 (1991).

27. J. R. Probert-Jones, "Resonance component of backscattering by dielectric spheres," J. Opt. Soc. Am. A **1**, 822-830 (1984).